Study on aero-acoustic structural interactions in fan-ducted system

Yan-kei CHIANG[1]; Yat-sze CHOY[2]; Li CHENG[3]; Shiu-keung TANG[4]

[1, 2, 3] Department of Mechanical Engineering, The Hong Kong Polytechnic University, HKSAR.

[4] Department of Building Service Engineering, The Hong Kong Polytechnic University, HKSAR.

ABSTRACT

Mitigation of sound radiation from subsonic axial fan in the fan-ducted system at low frequencies remains a technical challenge. Traditional dissipative approach such as absorption material often requires sufficiently long attenuation path for desirable noise reduction performance. More advanced passive control technology such as membrane housing which relies on vibro-acoustic coupling mechanism works effectively on the attenuation of the first and second blade passage frequency in case of steady flow. However, the performance of such device which is composed of thin membrane may be affected by unsteady flow field. This study examined the interaction between vortex unsteady motion, a tensioned membrane housing of finite length and axial fan with dipole nature using the matched asymptotic expansion technique and potential theory. A two-dimensional numerical model is established to explore the sound radiation of each components and the performance of the membrane housing for controlling sound radiation from axial fan in the present of vortex inside uniform mean flow. The results show that there is higher chance of sound amplification when a vortex stream is closer to the light membrane under weak mean flow speed. Under the condition of weak mean flow speed, the sound radiation from the membrane is also amplified when the cavity height is shallower. The result is beneficial for the design of the device of membrane housing.

Keywords: Axial fans, Flow-induced noise generation in ducts and pipes
I-INCE Classification of Subjects Number(s): 26.1

1. INTRODUCTION

The operation of the air conditioning and ventilation system causes noise problem especially at the low frequency regime although such facilities could improve the comfort quality of human being. The central air conditioning and ventilation system normally composed of fan and duct which is so called fan-ducted system. The operation of the fan creates vibration noise due to rotating unbalance or friction between rotating parts, and also the aerodynamic noise. Traditionally, low frequency noise in the fan-ducted system could be attenuated by different passive approaches such as duct lining (1, 2) and the technology of expansion chamber (3). Duct lining with sufficient length can perform well in the range of medium to high frequencies but for low frequencies, the attenuation of noise is ineffective due to the inherent high magnitude of characteristics impedance of sound absorption material. And it would cause environmental and hygiene problems when using fibrous absorber (4, 5). Besides, the device of expansion chambers is traditionally bulky in order to provide an acceptable acoustical performance for low frequencies noise. It causes unavoidable pressure drop due to the change of cross sectional area when there is flow. In order to eliminate the pressure drop and achieve a broadband noise reduction for the duct system, Huang (6) proposed the concept of drum-like silencer which composed of two light membranes under high tension covered with the side-branch cavities. It can achieve the low frequencies noise attenuation by the effect of membrane vibration. The performance of the drum-like silencer without and with mean flow is studied experimentally (7, 8).

At low rotating speed of fan, the dominant sound generated is caused by fluctuating forces due to the interaction of flow turbulence with the blades or fan casing (9). In addition, an unsteady flow

[1] kidencyk@gmail.com
[2] mmyschoy@polyu.edu.hk
[3] mmlcheng@polyu.edu.hk
[4] shiu-keung.tang@polyu.edu.hk

would be generated when the fan is operating. This can be normally found from the air handling unit. Baade (10) showed that the fan noise has feature of acoustic dipole and the unsteady flow, which is regarded as flow turbulent eddies (11), composed of the nature of acoustic dipole and quadrupole (12). For the unsteady flow, Lamb (13) showed that the former one is caused by the fluid force due to the fore-and-aft displacement of fluid created by the vibration of cylinder. The latter one, stated by Powell (14), is the sound of free aerodynamic flows generated by the momentum fluctuations that accelerate the fluid particle in order to attain the local velocity in the shear layer. It is believed that acoustic dipole would be dominant at the fan when the Mach number is low. For controlling noise in fan-ducted system, many researchers investigated different approach to reduce the fan noise in the propagation path such as duct lining with uniform or non-uniform alignment (15, 16) and membrane absorber box (17, 18). However, very little attention is paid on controlling the noise directly at the sound source. Recently, Liu et. al (19) investigated the reactive nose control method by suppressing the sound radiation from fan with dipole nature directly. They designed a device which composed of two tensioned membranes with side-branch cavities to house the dipole sound source. A theoretical model with uniform mean flow was also established to study the performance of such a device. Due to dealing with the complicated vibro-acoustic coupling problem between the membrane and acoustic waves as well as dipole source, they simplified the model by considering steady fluid flow in fan-ducted system. However, the fan induced fluid flow field is unsteady. In addition, when turbulent flow interacts with the flexible walls, the loading on the membrane varies with time that may cause significant change of the membrane motion. Hence, it may also probably affect the performance of such membrane housing device. Therefore the current study focuses on examining the interaction between the membrane, acoustics waves and unsteady flow in the fan-ducted system. The numerical model in the time domain is to be established in order to have more understanding the physics behind. And the result will be beneficial to assess the performance of membrane housing device to control fan noise with the excitation of turbulence.

In what follows, Section 2 focuses on the theoretical model development of cavity backed silencer installed along the fan-ducted system with unsteady flow. The numerical results and discussions of the vortex dynamics associated with different dipole strengths at different uniform flow speeds, at different initial vortex height, as well as the sound radiations are described in Section 3. Finally, main conclusions are made in Section 4.

2. THEORETICAL MODEL DEVELOPMENT

In this section, the theoretical formulations for the predictions of membrane vibrations, unsteady vortex motions and the far-field sound radiations are outlined. A two-dimensional infinitely long duct model that shown as Fig. 1 with passive noise control device which contained two flexible membranes, a point vortex with circulation Γ, mean flow speed U and a dipole source is established. It consists of a rectangular duct with height a and a silencer with two flexible boundaries backed by cavities of length L and depth h. A vortex is initially located at the upstream of the duct (x_0, y_0) and the dipole source is at x=0, y=0.5a.

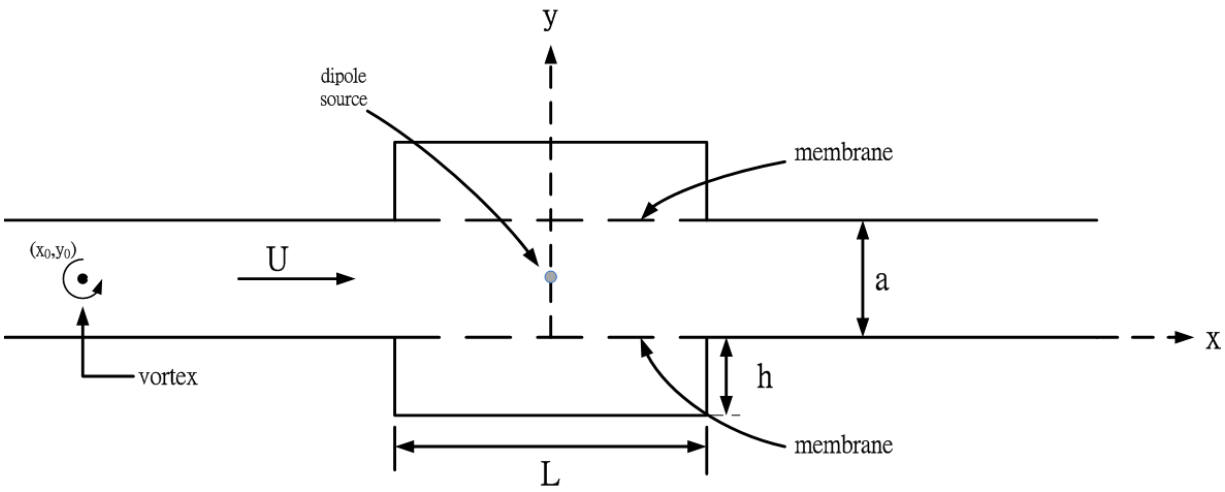

Figure 1 - 2D theoretical model of dipole source control with two flexible panels with unsteady fluid flow

The flexible panels with two side-branch backed cavities are assumed to be very thin and the bending stiffness is ignored. The motion of the lower and upper tensioned membranes are governed by the following equations

$$m\frac{\partial^2\eta_l}{\partial\tau^2}=T\frac{\partial^2\eta_l}{\partial x'^2}-D\frac{\partial\eta_l}{\partial\tau}-(p_{l,duct}-p_{l,cavity}) \tag{1}$$

and

$$m\frac{\partial^2\eta_u}{\partial\tau^2}=T\frac{\partial^2\eta_u}{\partial x'^2}-D\frac{\partial\eta_u}{\partial\tau}-(p_{u,cavity}-p_{u,duct}) \tag{2}$$

where the suffices *u* and *l* are representing the quantities related to the upper and lower membrane respectively, *m* is the mass density of the membrane, *T* is the tension of membrane per unit length, *D* is regarded as the damping coefficient, η denotes the membrane displacement, τ is time, *x'* denotes the x-direction for the membrane section, $p_{l,duct}$ and $p_{u,duct}$ are duct-side acoustic pressure acting on the lower and upper membrane respectively, $p_{l,cavity}$ and $p_{u,cavity}$ are cavity-side acoustic pressure acting on the lower and upper membrane respectively.

The duct-side fluid pressure, $p_{l,duct}$ and $p_{u,duct}$, are deduced by the linearized Bernoulli relationship and the near field incompressible velocity potential (20), ϕ which is attributed to the membrane vibrations ϕ_m, dipole source ϕ_d, vortex ϕ_v and mean flow $\phi_f=Ux$. The incompressible velocity potential of the acoustic dipole source inside the duct is deduced by modelling it as a hydrodynamic doublet as the dipole source and doublet are both described as the composition of two sources that one is having an inward volume flow rate and the other one having the outward volume flow rate with same magnitude. By the potential theory (21), the fluid potential is given as the following expression at any point *(x,y)* inside the duct

$$\phi(x,y,\tau)=\phi_m+\phi_d+\phi_v+\phi_f+\gamma(\tau) \tag{3}$$

where

$$\phi_m=\frac{1}{2\pi}\int_{-L/2}^{L/2}\left(\frac{\partial\eta_l}{\partial\tau}+U\frac{\partial\eta_l}{\partial x'}\right)\log\left[\cosh\left(\frac{\pi(x-x')}{a}\right)-\cos\left(\frac{\pi(y-\eta_l)}{a}\right)\right]dx'$$
$$-\frac{1}{2\pi}\int_{-L/2}^{L/2}\left(\frac{\partial\eta_u}{\partial\tau}+U\frac{\partial\eta_u}{\partial x'}\right)\log\left[\cosh\left(\frac{\pi(x-x')}{a}\right)+\cos\left(\frac{\pi(y-\eta_u)}{a}\right)\right]dx',$$

$$\phi_d=\frac{\mu(\tau)}{4\pi}\log\left[\frac{\left(e^{\frac{\pi x}{a}}\cos\frac{\pi y}{a}-e^{\frac{\pi(x_d-\varepsilon)}{a}}\cos\frac{\pi y_d}{a}\right)^2+\left(e^{\frac{\pi x}{a}}\sin\frac{\pi y}{a}-e^{\frac{\pi(x_d-\varepsilon)}{a}}\sin\frac{\pi y_d}{a}\right)^2}{\left(e^{\frac{\pi x}{a}}\cos\frac{\pi y}{a}-e^{\frac{\pi(x_d+\varepsilon)}{a}}\cos\frac{\pi y_d}{a}\right)^2+\left(e^{\frac{\pi x}{a}}\sin\frac{\pi y}{a}-e^{\frac{\pi(x_d+\varepsilon)}{a}}\sin\frac{\pi y_d}{a}\right)^2}\right]$$
$$+\frac{\mu(\tau)}{4\pi}\log\left[\frac{\left(e^{\frac{\pi x}{a}}\cos\frac{\pi y}{a}-e^{\frac{\pi(x_d-\varepsilon)}{a}}\cos\frac{\pi y_d}{a}\right)^2+\left(e^{\frac{\pi x}{a}}\sin\frac{\pi y}{a}+e^{\frac{\pi(x_d-\varepsilon)}{a}}\sin\frac{\pi y_d}{a}\right)^2}{\left(e^{\frac{\pi x}{a}}\cos\frac{\pi y}{a}-e^{\frac{\pi(x_d+\varepsilon)}{a}}\cos\frac{\pi y_d}{a}\right)^2+\left(e^{\frac{\pi x}{a}}\sin\frac{\pi y}{a}+e^{\frac{\pi(x_d+\varepsilon)}{a}}\sin\frac{\pi y_d}{a}\right)^2}\right],$$

$$\phi_v=\frac{\Gamma}{2\pi}\tan^{-1}\left[\tan\left(\frac{\pi(a-y_v+y)}{2a}\right)\tanh\left(\frac{\pi(x-x_v)}{2a}\right)\right]$$
$$+\frac{\Gamma}{2\pi}\tan^{-1}\left[\tan\left(\frac{\pi(a-y_v-y)}{2a}\right)\tanh\left(\frac{\pi(x-x_v)}{2a}\right)\right]$$

and the linearized Bernoulli relationships are

$$p_{l,duct}=-\rho_0\left(\frac{\partial\phi}{\partial\tau}+U\frac{\partial\phi}{\partial x}\right)\Big|_{y=\eta_l}\quad\text{and}\quad p_{u,duct}=-\rho_0\left(\frac{\partial\phi}{\partial\tau}+U\frac{\partial\phi}{\partial x}\right)\Big|_{y=\eta_u} \tag{4}$$

where ρ_0 is the fluid density, $\mu(\tau)$ is the magnitude of volume flow rate created by the source and sink, $\gamma(\tau)$ is a time function that is found by the matching procedure, ε denotes the half of distance between the source and sink that form the doublet, (x_d, y_d) is the location of the doublet and (x_v, y_v) is the vortex position.

For the cavity-side fluid pressure, $p_{l,cavity}$ and $p_{u,cavity}$, the acoustic pressure distribution inside the cavity and along the flexible boundaries is therefore estimated by Finite Difference Time Domain (22) (FDTD). The FDTD is developed based on two governing equations of the motion of air particles, which are the conservation of momentum

$$\nabla p + \rho_0 \frac{\partial \vec{v}}{\partial \tau} = 0 \tag{5}$$

and the continuity equation

$$\frac{\partial p}{\partial \tau} + \rho_0 c^2 \nabla \cdot \vec{v} = 0 \tag{6}$$

where p represents the acoustic pressure, c is the speed of sound and $\vec{v}$ is the vector particle velocity which contains two components, the particle velocity in x-direction v_x, and the one in y-direction v_y.

The sound wave propagating inside the cavity is approximate by applying the second-order centered difference operators to discretize the first-order derivatives in Eq. (5) and (6). The formulations of FDTD determines the acoustical pressure and particle velocity at the grid positions where Δx and Δy are the spatial step size in x-direction and y-direction respectively, $\Delta\tau$ denotes the temporal step size, i and j are indictor of spatial points for x- and y-axis respectively, n is the indicator of time instant. The discretized two-dimensional FDTD basic equations in a Cartesian grid are expressed as follows

$$v_x^{n+0.5}\left(i+\frac{1}{2}, j\right) = v_x^{n-0.5}\left(i+\frac{1}{2}, j\right) - \frac{\Delta\tau}{\rho_0 \Delta x}\left[p^n(i+1, j) - p^n(i, j)\right] \tag{7}$$

$$v_y^{n+0.5}\left(i, j+\frac{1}{2}\right) = v_y^{n-0.5}\left(i, j+\frac{1}{2}\right) - \frac{\Delta\tau}{\rho_0 \Delta y}\left[p^n(i, j+1) - p^n(i, j)\right] \tag{8}$$

$$p^{n+1}(i, j) = p^n(i, j) - \frac{\rho_0 c^2 \Delta\tau}{\Delta x}\left[v_x^{n+0.5}\left(i+\frac{1}{2}, j\right) - v_x^{n+0.5}\left(i-\frac{1}{2}, j\right)\right] - \frac{\rho_0 c^2 \Delta\tau}{\Delta y}\left[v_y^{n+0.5}\left(i, j+\frac{1}{2}\right) - v_y^{n+0.5}\left(i, j-\frac{1}{2}\right)\right] \tag{9}$$

The vortex dynamics is therefore predicted by calculating its velocities for both x- and y-direction, which are denotes as u_x and u_y respectively. The vortex velocities are deduced by the use of the velocity potential of Eq. (3) and the following expressions

$$u_x = \frac{\partial \phi(x, y, \tau)}{\partial x} \quad \text{and} \quad u_y = \frac{\partial \phi(x, y, \tau)}{\partial y}.$$

Without dipole, due to the interaction between the membrane and the vortex, the far-field acoustic pressure radiations can be deduced by applying the matched asymptotic expansion technique between the wave equation and the incompressible fluid potential of Eq. (3). The wave equation for far-field acoustic radiation in plane wave is (23)

$$\left(1 - M^2\right)\frac{\partial^2 \phi}{\partial x^2} - \frac{2M}{c_0}\frac{\partial^2 \phi}{\partial x \partial \tau} - \frac{1}{c_0^{\,2}}\frac{\partial^2 \phi}{\partial \tau^2} = 0 \tag{10}$$

where M denotes the Mach number, U/c_0.

The sound radiations pressure in far-field which was described by Tang (24) is therefore expressed as the follows

$$p_{+\infty} = -\frac{\rho_0}{1+M}\left[-\frac{\Gamma}{2a}\frac{\partial y_v}{\partial \tau} + \frac{c}{2a}\int_{-L/2}^{L/2}\frac{\partial}{\partial \tau}\left(\eta_u - \eta_l\right)dx'\right] \tag{11}$$

3. NUMERICAL RESULTS AND DISCUSSIONS

For the sake of convenience, the parameters such as length, velocity and density are normalized by the following quantities, which are duct height, a, circulation, Γ/a, and air density, ρ_0, respectively. The length of membrane is set to be 2, located from -1 to 1. The circulation of vortex remains constant and the initial position of the vortex is placed at x_0=-10.

3.1 Effect of vortex

With damping *D*=1, mass and tension of membrane is set to be $m = 100,\ T = 100$. Fig. 2 shows the comparison of the vortex paths with different doublet strengths at mean flow speed $U = 0$ with $h = 0.5$. When the vortex gets close to the doublet position at $x = 0$, there is a drop of vortex path due to the effects of fluid field created by the doublet. By introducing a doublet $\mu = 3100$(dashed line) or $\mu = 6200$(dash-dot line), the position of vortex drops downward due to the effect of fluid field by the doublet. The level of dropping of the vortex increases with the strength of the doublet.

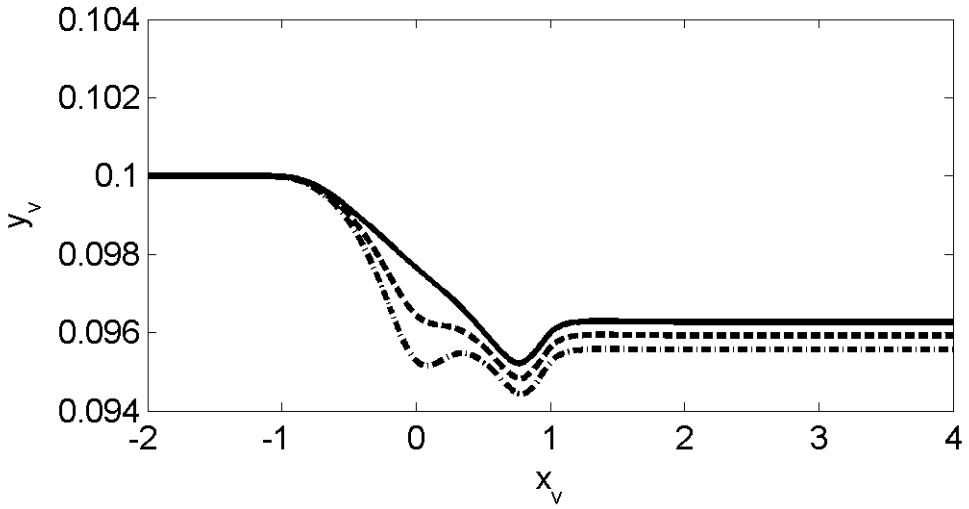

Figure 2 - Effects of doublet strength on vortex motion. (—) $\mu = 0$; (---) $\mu = 3100$; (–•–) $\mu = 6200$.

Fig. 3 shows the results of vortex motion with different initial vortex height at mean flow speed *U*=1.0 with μ=0 and *h*=0.5. When the initial vortex height is far away from the centerline of the duct, the variation of the vortex motion is more significant (solid line). In this case, the motion of the vortex is mainly affected by the lower membrane vibrations. On the other hand, when the vortex is initially located closer to the centerline of the duct, the variation of the vortex position is less significant (dashed line) due to equalization of released pressure from the upper and lower flexible membrane. The results are consistent with the findings of Tang (24) that a weaker vortex velocity in y-direction is obtained with the increase of the initial vortex position. In order to further study the vortex path at different flow speed when the vortex is closed to the membrane, it is located at y_0=0.1.

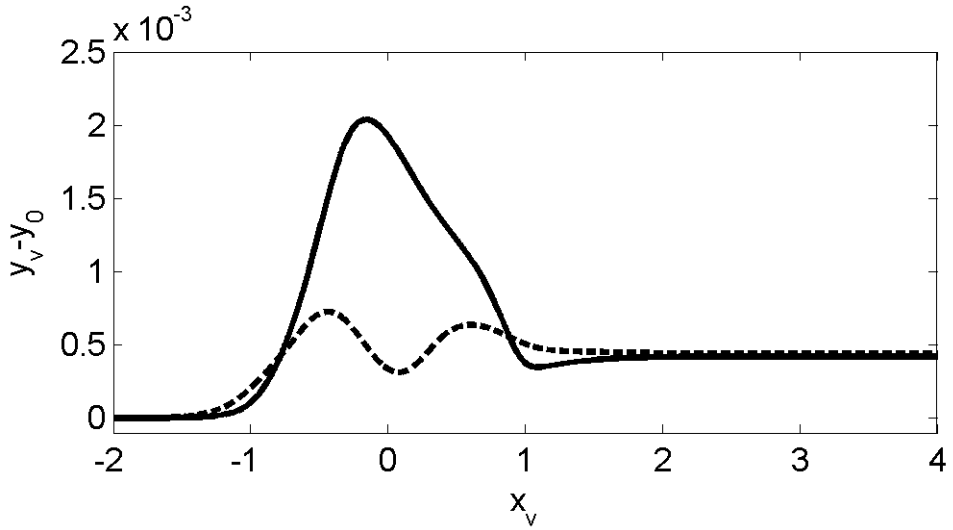

Figure 3 - Effects of initial vortex position on vortex motion. (—) $y_0 = 0.1$; (---) $y_0 = 0.3$.

Fig. 4 shows its vortex path at different flow speed when the doublet strength is fixed to be $\mu = 3100$. Fig. 4(a) and 4(b) show the results for the cavity height of 0.5 and 1.0 respectively. It shows that variation of the vortex paths becomes smaller when the mean flow speed is increased due to the phases of the membrane vibration when the vortex starts to interact with the membrane. The pattern of the vortex path appears to be similar with different cavity height but its magnitude in variation is increased with increasing cavity height. These results are mainly caused by the different responses of membrane vibrations as shown in Fig. 5 which is describing the membrane vibrating for mean flow speed equals to 1.0. The acoustic pressure distributions inside the backed-cavities are not the same with different cavity depths, thus, the acoustic loadings acting on the flexible boundaries for the cavity-side is different leading different membrane vibrations as shown in Fig 6. Therefore, the vortex dynamics are influenced by the cavity depth indirectly through the changes of flexible boundaries vibrations.

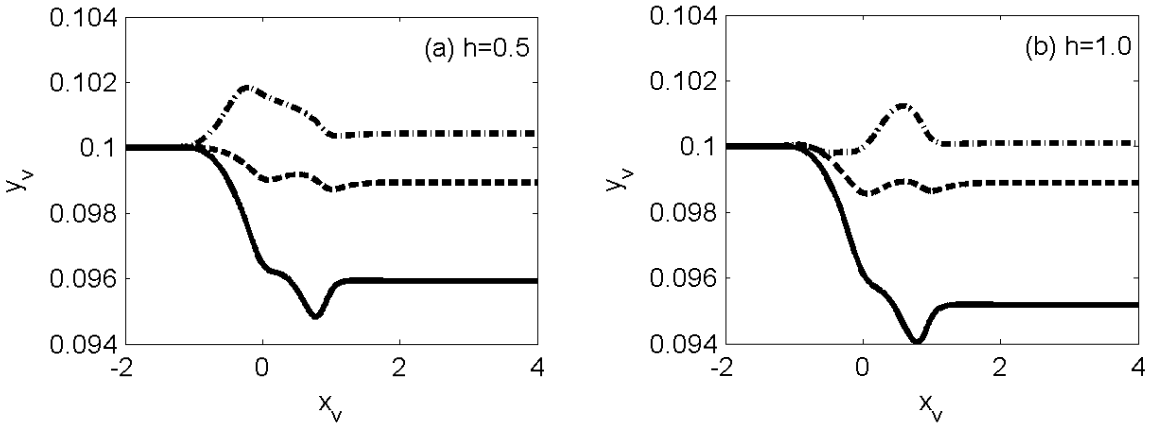

Figure 4 - Effects of mean flow speed on vortex motion. (a) $h = 0.5$; (b) $h = 1.0$.
(—) $U = 0$; (---) $U = 0.5$; (–•–) $U = 1.0$.

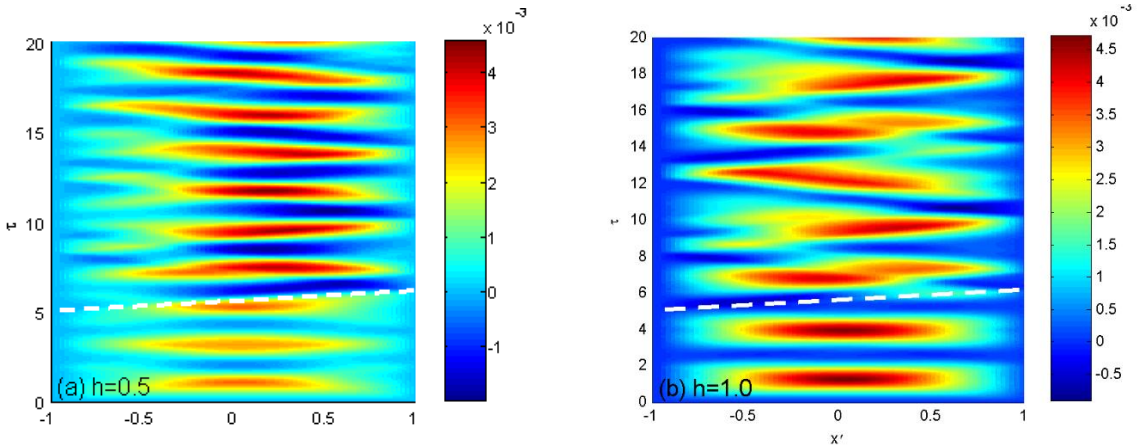

Figure 5 - Variations of lower membrane displacement at different time for *U*=1.0.
(a) $h = 0.5$; (b) $h = 1.0$.

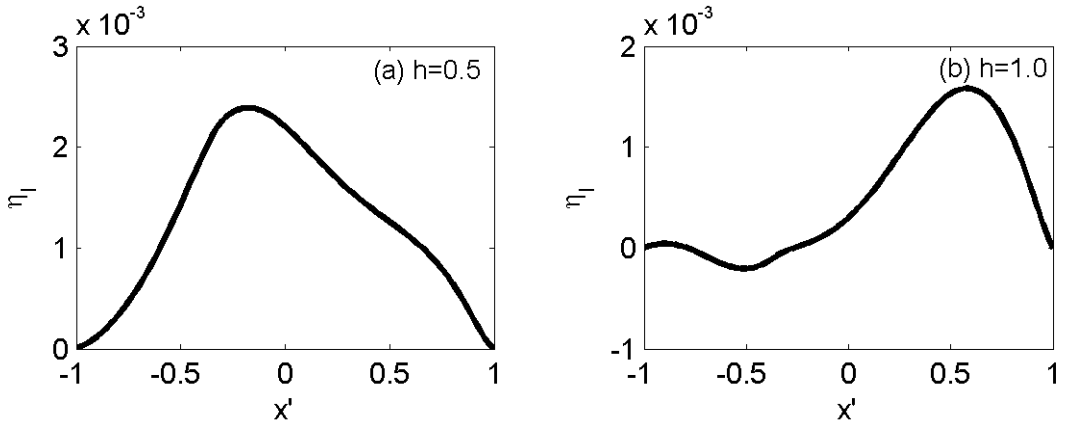

Figure 6 - Lower membrane displacement for *U*=1.0. (a) *h*=0.5; (b) *h*=1.0.

3.2 Effect of far-field sound pressure radiation

For the far-field sound radiation, Fig. 7(a) and 7(b) show the far-field acoustic pressure radiations for the model with backed-cavities height $h = 0.5$ and 1.0 respectively. When there is no mean flow (solid line) in both Fig. 7(a) and 7(b), the downstream sound radiation is not significant for the time $\tau < 13.5$ where the vortex is still at the upstream of the duct. After the vortex has engaged to the membrane section at $\tau > 13.5$, there is an increase in the acoustic pressure radiation as the membrane vibrates with a larger amplitude due to the vortex excitation. For the case with mean flow speed $U = 0.5$ (dashed line), sound is radiated before the vortex interact with the membranes, due to the membrane vibrations excited by the mean flow. At the time that the vortex has already passed the membrane section, same as the case of $U = 0$ that an increase of radiated acoustic pressure is observed due to the excitation created by the vortex on the membranes. However, there is less significant increase in sound pressure magnitude with higher speed of mean flow after the vortex has engaged to the membranes (dash-dot line). The acoustic pressure is mainly generated by two components, which are the vortex and membranes. Fig. 7 demonstrates that the membranes monopole radiation is always dominant. Although the vortex sound is less dominant, the vortex excites the membranes to oscillate vigorously to cause a larger pressure radiation once it starts engaging to the membrane section for $U \leq 1$ and $h = 0.5$. When the mean flow speed is higher, the effect of vortex excitation is less significant as there is less time for the vortex to interact with the membranes. The spectrum of far-field sound radiations for the case with $h = 1.0$ as shown in Fig. 7(b) is different when comparing with a smaller cavity depth in Fig. 7(a). With different cavity heights, the cavity pressure distributions are different such that the acoustic loadings applied on the membranes are not the same. Thus, the vortex dynamics and membrane vibrations are different, as shown in Fig. 4 and 5, with different cavity height as they both depend on the pressure loadings acting on the membranes. Therefore, the spectrum of sound radiation due to the membrane oscillations and transverse acceleration of vortex in downstream is different.

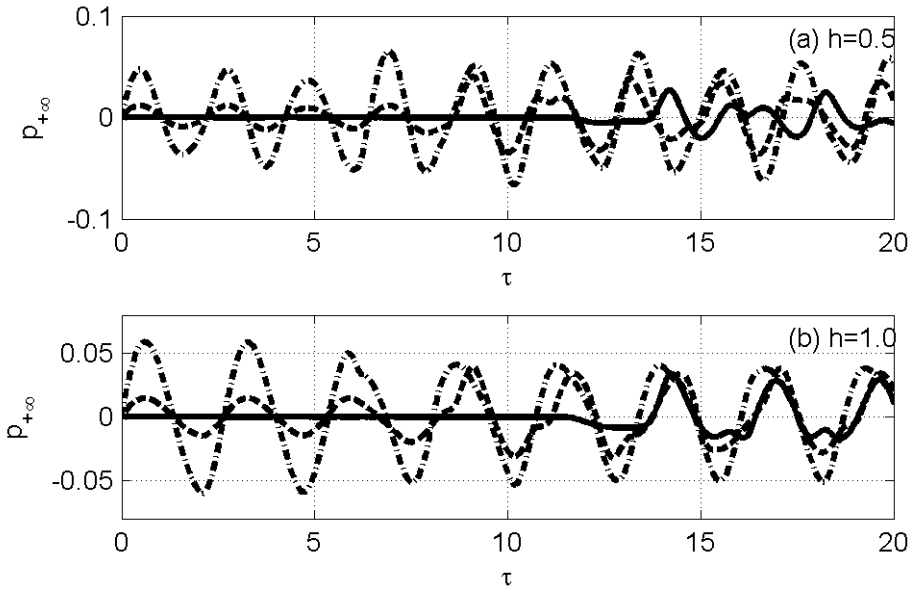

Figure 7 - Time variations of downstream sound pressure radiation with different mean flow.

(a) $h = 0.5$; (b) $h = 1.0$. (—) $U = 0$; (---) $U = 0.5$; (–•–) $U = 1.0$.

Fig. 8 illustrates that the far-field acoustic pressure radiated in the model with $U = 1.0$, $h = 0.5$ and the initial vortex height is y_0=0.1 and 0.3 respectively. It is observed that the vortex is initially located closer to the centreline of the duct at y_0=0.3 (dashed line), the sound radiation due to vortex excited membrane vibrations is relatively smaller when comparing that with y_0=0.1 (solid line). The reduction of far-field sound pressure radiation with the increase of the initial vortex height is obtained due to the smaller vortex transverse acceleration caused by the pressure equalization between two membranes. Moreover, when the initial vortex height is closer to the centerline of the duct, the ability for the vortex to excite the lower membrane oscillations is reduced due to the larger distance between the vortex and lower membrane. The sound radiations due to vortex excitation are thus reduced.

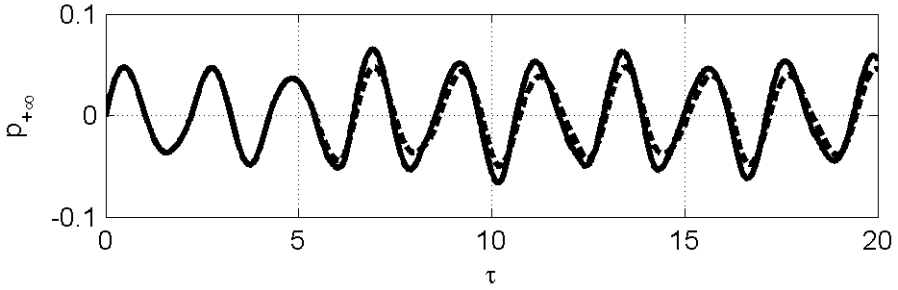

Figure 8 - Time variations of downstream sound pressure radiation with different initial vortex height.

(—) $y_0 = 0.1$; (---) $y_0 = 0.3$.

4. CONCLUSIONS

Theoretical analyses have been conducted to understand the fluid-structural interactions under the unsteady flow. The time-varying vortex dynamics and far-field time domain sound pressure radiations has been investigated numerically with the changes of several parameters such as the mean flow speeds and height of backed-cavity. Major conclusions can be summarized as follows:

(1) A two-dimensional theoretical formulation has been established to examine the performance of silencing device with tensioned membrane covered with a cavity to suppress the axial flow fan with the unsteady flow in the time domain.

(2) With the existence of doublet which simulates the axial fan, it creates a change of volume flow rate of the fluid, and thus, affects the flow field of surrounding fluid. The results illustrate that the effects on the vortex drop caused by the doublet is obvious when the vortex is propagating at x is around -0.4 to 0.4. Out of this range, the variations of the vortex paths with and without doublet are similar. It shows that the vortex dynamics at $x < -0.4$ or $x > 0.4$ are mainly associated with the vibrations of the flexible structures which has strong interaction with the doublet.

(3) Without considering the doublet sound radiation, the far-field sound radiations are mainly generated by two components: the membrane oscillations due to the vibration created rate change of the volumetric flow and vortex excitation due the transverse acceleration of vortex. From the observations, the effect on the sound radiations due to the vortex excitation is less significant for a higher mean flow, U=1.0, as the oscillations of membranes driven by the uniform flow are larger in amplitude comparing with U=0 and 0.5. Moreover, the time that allowing the vortex to excite the membrane is less as the vortex velocity in x-direction increases with the mean flow speed. Therefore, when the vortex passes over the membrane sections, the acoustic pressure radiation in downstream amplified due to vortex excitation is less dominant.

ACKNOWLEDGEMENTS

The first author thanks the Hong Kong Polytechnic University for the research studentship and General Research Grant from the Hong Kong SAR government (B-Q33E).

REFERENCES

1. Beranek LL, Vér IL. Noise and vibration control engineering : principles and applications. New York: John Wiley & Sons, Inc.; 1992.
2. Ingard KU. Notes on sound absorption technology. Poughkeepsie, NY: Noise Control Foundation; 1994.
3. Munjal ML. Acoustics of ducts and mufflers with application to exhaust and ventilation system design. New York: Wiley; 1987.
4. Fuchs HV. From Advanced Acoustic Research to Novel Silencing Procedures and Innovative Sound Treatments. ACUSTICA. 2001a;87:407-13.
5. Fuchs HV. Alternative Fibreless Absorbers - New Tools and Materials for Noise Control and Acoustic Comfort. ACUSTICA. 2001b;87:414-22.
6. Huang L. A theoretical study of duct noise control by flexible panels. The Journal of the Acoustical Society of America. 1999;106(4):1801-9.
7. Choy YS, Huang L. Experimental studies of a drumlike silencer. The Journal of the Acoustical Society of America. 2002;112(5):2026-35.
8. Choy YS, Huang L. Effect of flow on the drumlike silencer. The Journal of the Acoustical Society of America. 2005;118(5):3077-85.
9. Kemp NH, Sears WR. Aerodynamic Interference Between Moving Blade Rows. Journal of the Aeronautical Sciences (Institute of the Aeronautical Sciences). 1953;20(9):585-97.
10. Baade PK. Effects of Acoustic Loading on Axial Flow Fan Noise Generation. Noise Control Eng Noise Control Engineering. 1977;8(1).
11. Crighton DG. Radiation from vortex filament motion near a half plane. Journal of Fluid Mechanics. 1972;51(02):357-62.
12. Powell A. Theory of Vortex Sound. The Journal of the Acoustical Society of America. 1964;36(1):177-95.
13. Lamb H. Hydrodynamics. New York: Dover publications; 1945.

14. Powell A. On Aerodynamic Sound from Dilatation and Momentum Fluctuations. The Journal of the Acoustical Society of America. 1961;33(12):1798-9.
15. Parrott TLWWRUSNA, Space Administration S, Technical Information B. Comparison of measured and calculated mode redistribution associated with spinning mode transmission through circumferentially segmented lined ducts. Washington, D.C.; Springfield, Va.: National Aeronautics and Space Administration, Scientific and Technical Information Branch ; For sale by the National Technical Information Service]; 1983.
16. Bi W, Pagneux V, Lafarge D, Aurégan Y. An improved multimodal method for sound propagation in nonuniform lined ducts. The Journal of the Acoustical Society of America. 2007;122(1):280-90.
17. Ackermann U, Fuchs HV, Rambausek N. Sound absorbers of a novel membrane construction. Applied Acoustics. 1988;25(3):197-215.
18. Frommhold W, Fuchs HV, Sheng S. Acoustic Performance of Membrane Absorbers. Journal of Sound and Vibration. 1994;170(5):621-36.
19. Liu Y, Choy YS, Huang L, Cheng L. Noise suppression of a dipole source by tensioned membrane with side-branch cavities. The Journal of the Acoustical Society of America. 2012;132(3):1392-402.
20. Vallentine HR. Applied hydrodynamics. London: Butterworths; 1967.
21. Currie IG. Fundamental Mechanics of Fluids, Third Edition: Taylor & Francis; 2002.
22. Botteldooren D. Finite‐difference time‐domain simulation of low‐frequency room acoustic problems. The Journal of the Acoustical Society of America. 1995;98(6):3302-8.
23. Mechel FP, Munjal L. Formulas of Acoustics: Springer; 2008.
24. Tang SK. Vortex sound in the presence of a low Mach number flow across a drum-like silencer. The Journal of the Acoustical Society of America. 2011;129(5):2830-40.